6 March 2017

Using Global Tide Gauge Data to Validate and Improve the Representation of Extreme Sea Levels in Flood Impact Studies

J.R. Hunter[1], P.L. Woodworth[2], T. Wahl[3] and R.J. Nicholls[4]

1. Antarctic Climate & Ecosystems Cooperative Research Centre, University of Tasmania, Private Bag 80, Hobart, Tasmania 7001, Australia

2. National Oceanography Centre, Joseph Proudman Building, 6 Brownlow Street, Liverpool L3 5DA, United Kingdom

3. Department of Civil, Environmental and Construction Engineering and Sustainable Coastal Systems Cluster, University of Central Florida, 12800 Pegasus Drive, Orlando 32816-2450, USA

4. Faculty of Engineering and the Environment, University of Southampton, Southampton SO17 1BJ, United Kingdom

Corresponding author: P.L. Woodworth (plw@noc.ac.uk)

Abstract

The largest collection of tide gauge records assembled to date, called GESLA-2, has been used to provide reliable extreme sea level parameters at 655 locations around the world. This has enabled a rigorous assessment of the European Union-funded DINAS-COAST (D-C) data set of extreme sea level

information for the global coastline that has been used in many published flood impact studies. We find the D-C extreme levels to be generally both too high, compared to those from GESLA-2, and too flat, when plotted as a function of return period. This leads to an over-estimation of the probability of extreme sea levels in the present day for most locations around the world, and also to an over-estimation of the probability of extreme sea levels in the future as sea level rises. A detailed impact study is conducted for the world's largest coastal cities following the approach of Hallegatte et al. (2013), resulting in similar conclusions for these particular locations. We suggest that most previous studies that have relied upon D-C information should be re-assessed in the light of these findings, using more recent modelling-based estimates of extreme sea level information.

Keywords: Extreme sea level parameters; GESLA-2 tide gauge data set; DINAS-COAST data set; Major coastal cities flood risk.

1. Introduction

As climate changes, and as sea level rises, coastal impacts are expected due to an increase in the likelihood of flooding. There will be costs associated with flood damage, human impacts and the need for modified coastal infrastructure and adaptation. Such impacts have been assessed at local to global scales using knowledge of the distribution of coastal populations and assets, coastal topography, estimates of present and future coastal adaptation, and plausible projections of future increases in mean and extreme sea levels (Nicholls, 2010). Extreme level parameters are needed in such studies in order to estimate present-day and future changes in the likelihood of extreme events as sea level rises.

A notable achievement in this area of research has been the development of the Dynamic and Interactive Vulnerability Assessment (DIVA) model (Hinkel and Klein, 2009; Hinkel et al., 2014) which has been employed to estimate the global costs of coastal impacts under scenarios of climate, sea level and socio-economic change, and has been influential in review processes such as the Intergovernmental Panel on Climate Change Fifth Assessment Report (IPCC AR5). The parameterisation of the likelihood of extreme sea levels used in most DIVA assessments was developed more than a decade ago by the European Union (EU)-funded DINAS-COAST (Dynamic and Interactive Assessment of National, Regional and Global Vulnerability of Coastal Zones to Sea-Level Rise, hereafter D-C) project (Vafeidis et al., 2008).

In this paper, we report on a rigorous assessment of the extreme level parameterisations in D-C by means of an independent quasi-global data set of extreme sea level information obtained by tide gauges. This tide gauge data set is the largest ever to have been assembled. For each tide gauge record spanning at least 20 years, we have computed extreme sea level parameters, suitable for comparison to those in D-C at the same locations, and thereby providing as complete as possible a validation of the D-C data set.

This assessment demonstrates that there are important deficiencies in the D-C data, as might be expected in a relatively old dataset. Nevertheless, we feel that it is useful to clarify these deficiencies as the D-C data has been used extensively in earlier impact and adaptation research of coasts (e.g. McLeod et al., 2010; Hansen et al., 2011; Nicholls et al., 2011; Pardaens et al., 2011; Bosello et al., 2012; Hallegatte et al., 2013; Hinkel et al., 2010, 2014; Brown et al., 2016; Diaz, 2016), including in the IPCC AR5 Working Group II (Wong et al., 2014).

There is particular interest in knowing how coastal cities around the world may be subject to a greater frequency of flooding as sea level rises as they represent impact (and adaptation) hotspots.

77 Many of these cities have tide gauges nearby which have long records from which reliable extreme
78 sea level information may be extracted. We have used a flood risk model developed by Hallegatte et
79 al. (2013) to explore how improved estimates of extreme sea levels from these tide gauges, instead
80 of D-C information, change exposure and risk estimates at these locations for the present-day and
81 with future sea level rise.
82
83 In Section 2 below, we describe how extreme sea levels recorded by tide gauges are usually
84 parameterised as either Generalised Extreme Value (GEV) or the more restrictive Gumbel
85 distributions, and how parameters from the latter can be used to determine 1, 10, 100 and 1000
86 year return levels for comparison with the information in D-C. We then provide some background to
87 the development of the D-C data set and describe briefly how extreme sea level information is
88 parameterised within it. That is followed by an introduction to the quasi-global tide gauge data set
89 called GESLA-2 that we have used to validate the D-C values. Section 3 describes our main findings
90 from comparisons of D-C and GESLA-2 information. Section 4 then considers how different estimates
91 of changes in flood risk pertain to coastal cities, using either the D-C or GESLA-2 information. Section
92 5 refers to the implications for changes in the frequency of extreme sea levels with sea level rise,
93 and finally Section 6 summarises our conclusions.
94
95 ## 2. Extreme Levels and Data Sets
96
97 ### 2.1 Extreme Level Distributions
98
99 The highest sea level (also called the extreme sea level) recorded by a tide gauge in a year will vary
100 from year to year due to many factors. These factors include interannual changes in the ocean tide,
101 variations in the occurrence of large storm surges due to both tropical and extratropical cyclones
102 (e.g. von Storch and Woth, 2008; Khouakhi and Villarini, 2016), and fluctuations in mean sea level

(MSL) such as those that can be many decimetres in magnitude that occur in the tropical Pacific during El Niño Southern Oscillation (ENSO) events (Merrifield et al., 2013). The likelihood of a particular extreme level is commonly parameterised as a GEV distribution containing three parameters: the location, scale and shape parameters. The location parameter represents the height for some specific return period (e.g. the 1-year return level), the scale parameter gives the spread of extreme values from year to year (an e-folding distance in the vertical), and the shape parameter determines the upper tail of the distribution and describes the behaviour of the most unusual extreme events (Pugh and Woodworth, 2014). When the shape parameter is taken as zero, the GEV is reduced to a Gumbel distribution (Coles, 2001):

$$N = \frac{1}{R} = \exp\left(\left(\mu - h\right) / \lambda\right) \quad (1)$$

where N is the frequency of a level h being exceeded in a given year, which corresponds to a return period R and where μ and λ are the location and scale parameters respectively (the 'return period' is also called the 'average recurrence interval'). In most cases, the Gumbel distribution is found to be an adequate approximation of the GEV for return periods of 10s to 100s of years, i.e. for almost all observed extremes except for the most rare events (e.g. van den Brink and Können, 2011). Pairs of the 1, 10, 100 and 1000 year return period extreme levels above MSL ($H1, H10, H100$ and $H1000$) then have simple linear relationships such as:

$$\left(H100 - H1\right) / \lambda = \ln\frac{1}{1} - \ln\frac{1}{100} \quad (2)$$

where $H1$ is identical to the location parameter μ. In this situation, an 'extreme level curve', obtained by plotting extreme level versus the logarithm of the return period, is a straight line with a gradient that is proportional to the scale parameter.

This approach to our analysis of the tide gauge data from GESLA-2 is also appropriate for study of the extreme levels in the D-C data set which, it will be seen below, are largely consistent with having a Gumbel-like form for most of the world coastline.

2.2 DINAS-COAST and GESLA-2 Information

The D-C data set of extreme sea level information has a heritage in the earlier studies of the Global Vulnerability Assessment (GVA) (Hoozemans et al., 1993; Nicholls and Hoozemans, 2005). In these studies, present-day extreme sea levels around the global coastline are estimated by combining information on several oceanographic processes which result in high sea levels: the range of the ocean tide at the coast as represented by values of mean high water (MHW) above MSL taken from tide tables; the frequency and magnitude of storm surge (wind setup), simply modelled from wind conditions (which are inferred in turn from statistics of the wave climate) and estimates of the bottom slope and depth; and the possible changes in barometric pressure during storms. Other oceanographic processes, such as variability in the ocean circulation, are not included. This information on sea level variability is then used to derive present-day extreme sea level parameters, which are then combined with estimates of coastal subsidence and projections of MSL change in order to perform an impact assessment for some time in the future.

The D-C data set consists of a table of values of 1, 10, 100 and 1000 year extreme levels above MSL (i.e. the $H1, H10, H100$ and $H1000$ quantities mentioned above) for 12148 segments of the world coastline excluding Antarctica (Vafeidis et al., 2008; Wolff et al., 2016). The median distance

between nearest-neighbour segment centroids is 10.5 km. Pairs of H values can be used to determine the equivalent scale parameters according to Equation 2. In the results shown below, we have made use of $H1$ and $H100$ finding little difference when using $H10$ and $H1000$ (see below).

The tide gauge information comes from a data set called GESLA-2 that has been assembled from a number of national and international sea level databanks by Philip Woodworth (National Oceanography Centre, UK), John Hunter (University of Tasmania, Australia), Marta Marcos (University of the Balearic Islands, Spain), Melisa Menéndez (University of Cantabria, Spain) and Ivan Haigh (University of Southampton, UK). It is an update and extension of the GESLA (Global Extreme Sea Level Analysis) data set used by Menéndez and Woodworth (2010) and others. Although there are many individual contributions to GESLA-2, well over a quarter of its station-years are provided by the research quality data set of the University of Hawaii Sea Level Center. The GESLA-2 data set already has a reasonable geographical distribution (Figure SM1), although some coastline stretches have little or no coverage. It is planned to add other data in the future as it becomes available.

The data set presently contains 39151 station-years of information from 1355 station records (with some stations having alternative versions of the records provided by different sources) or typically 29 years per record, although the actual number of years varies from only 1 at several short-lived sites, to 167 in the case of Brest, France. The data set may be obtained from www.gesla.org. More detailed information may be found in Woodworth et al. (2017).

All the tide gauge data in GESLA-2 have hourly or more frequent sampling. Records will have had some form of quality control undertaken by the data providers. However, the extent to which that control will have been undertaken will inevitably vary between providers and probably with time. We are interested in non-tsunami ocean processes for comparison with D-C information. However, while some large tsunami signals and other data 'spikes' will have been removed from, or flagged in,

180 the tide-gauge records, some will undoubtedly remain. Therefore, in the first procedure to be
181 described (the one that is used for the final analyses), we apply a simple method for the rejection of
182 outlier annual maxima. We believe that the resultant extremes parameters are adequate for making
183 regional comparisons with D-C information. (There is a general question to do with the analysis of
184 extreme sea levels from tide gauge records, as to whether the most extreme events are reliably
185 recorded, see for example Section 7.3 of Pugh and Woodworth (2014). However, any locations
186 where there is significant loss of data on the highest extremes would likely yield extremes
187 distributions that are significantly non-Gumbel, leading to rejection by our iterative quality control
188 procedure. In the present application of the data set, which involves validation of the D-C data set
189 on a regional and global basis, we do not believe this question to be of major importance.)
190
191 We use annual extreme sea levels from the tide gauge records in GESLA-2. These extreme values are
192 the overall observed ones i.e. we are not concerned if the extremes arise primarily from variations in
193 the tide or in 'surge' or 'mean sea level' components. Gumbel parameters were computed from the
194 observed extremes by two methods.
195
196 The first method is based on that described by Hunter (2012). Prior to extremes analysis, the data
197 were detrended, and then ‘binned' so as to produce files with a minimum sampling interval of one
198 hour. Annual maxima were estimated using a declustering algorithm such that any extreme events
199 closer than 3 days were counted as a single event, and any gaps in time were removed from the
200 record. The method fits these annual maxima to a Gumbel distribution using the *ismev* package
201 (Coles, 2001, p. 48) implemented in the statistical language R (R Development Core Team, 2011).
202 Annual maxima were then rejected in an iterative fashion (with a maximum of 5 iterations) if they
203 fell outside a specified range (roughly 3.2-sigma) based on the estimated uncertainty range of the
204 Gumbel fit and the number of annual maxima (each time revising the earlier detrending process
205 using the reduced data set). If this process removed more than 15% of the original annual maxima,

206 that tide gauge record was not used. In addition, we removed four more records (from Balboa,
207 Newlyn, Brest and Roscoff) as further inspection showed the distribution of their extremes to be
208 clearly non-Gumbel in character. Records that survived these tests were assumed to have an
209 effective length equal to the number of annual maxima used in the final Gumbel fit.
210
211 Figure 1 provides examples of linear Gumbel fits using this procedure for six stations in quite
212 different locations. In each case, it shows annual maximum sea levels (above MSL) plotted versus
213 return period with the dashed lines giving 95% confidence intervals. The black squares are the
214 corresponding $H1$, $H10$ and $H100$ values (above MSL) for each location in the D-C data set, several of
215 which will be referred to below.
216
217 The number of annual maxima used in the final Gumbel fits is shown in Figure 2, and for further
218 analysis we require that this value be at least 20 years resulting in 655 stations. Figure 2 shows that
219 in most cases there are less than 60 annual maxima, although there is a long tail, with a largest value
220 of 123 years in the record from Stockholm, Sweden. (Brest does not provide our longest record for
221 analysis as many of its years of data are rejected in the above procedure.) Some of the peaks in this
222 distribution are artefacts of contributions to GESLA-2 from authorities with a large number of
223 stations, with each of their records spanning a similar period. For example, of the 27 stations in the
224 peak at 44 years, 11 are from Finland. The group with records of 60-65 years are primarily from the
225 USA.
226
227 It is generally accepted that return periods may be extrapolated out to around four times the
228 number of available annual maxima (see, for example, Pugh and Woodworth, 2014, page 323). We
229 have checked that the Gumbel fits provide formal errors which are consistent with this expectation.
230 We find the average errors (95% confidence level) of the 100-year return period levels to be ~0.15m
231 (7.2% of the levels themselves expressed relative to MSL) using the whole data set (655 stations), or

232 a little larger (~0.17m or 8.1%) for the 225 stations with only 20-30 annual maxima. This confirms
233 that the fits have value out to return periods of approximately a century, which is our main
234 timescale of interest.
235
236 A second method made use of independent software to obtain annual maximum sea level from each
237 year of data that was at least 75% complete. Care was taken not to include two annual maxima
238 occurring within a 3-day window at calendar year end/start. In these cases, the smaller of the two
239 maxima was excluded and an iterative search made for annual maxima at least 3 days apart in the
240 two individual years. Annual maxima were then expressed relative to the MSL linear trend for the
241 same years of data, so as to remove long-term changes in sea and land levels, in order to obtain
242 extremes relative to an "MSL datum" that is more akin to that implied in the D-C information. The
243 Gumbel parameters were then determined using the Matlab® *evfit* function.
244
245 The two methods resulted in almost the same Gumbel parameters and for the present study we
246 have used values from the first method only. The Gumbel location and scale parameters from that
247 method and their uncertainties are given in the Supplementary Material.
248
249 3. Comparisons of D-C and GESLA-2 Information
250
251 Figure 3(a) shows the extreme level information for the world coastline in the D-C data set. It shows
252 the distribution of the reciprocals of the scale parameters at each coastal location, as calculated
253 from the $H1$ and $H100$ levels and using Equation 2. (An exponential of the reciprocal of the scale
254 parameter determines the increase in the frequency of exceeding a given level using a Gumbel
255 distribution, as discussed further below.) These scale parameters are about 13% smaller than those
256 using $H10$ and $H1000$ (Figure SM2) which suggests that the D-C H values are not completely linear
257 (or Gumbel-like) but bend upwards at higher return periods (i.e. in a GEV there would be a small

positive shape parameter, see Coles (2001, p.50)). However, this 13% effect is not sufficiently large so as to invalidate our use of Gumbel parameterisations in the present analysis.

Most of the coastline in Figure 3(a) can be seen to be coloured red (i.e. the scale parameters at these locations are of the order of 0.05 m or less), although some sections of coast including NW Europe, the Atlantic coast of N America and the Russian Arctic are blue (i.e. scale parameters typically 0.2 m). For comparison, Figure 3(b) shows the reciprocals of the scale parameters for the 655 stations in the GESLA-2 data set that have at least 20 years of data. Although GESLA-2 does not extend to the entire global coastline, unlike D-C, there are sufficient points at which to perform a validation of the D-C information.

There can be seen to be some similarities between Figures 3(a) and 3(b), such as the sections of coast in blue for NW Europe and the Atlantic and Gulf coasts of N America. However, there are also differences, such as the Pacific coasts of N and S America which are all red in Figure 3(a), but are blue along the Canadian and Alaskan coasts in Figure 3(b). In addition, on the coasts of Australia and China there are generally more (and darker) blue dots in panel (b) than in (a).

In spite of the spatial limitations of the GESLA-2 data set, it has sufficient coverage to make a first general point: that the D-C data set contains scale parameters that are generally too small, or, in other words, contains sets of extreme level information ($H1$, $H10$, $H100$ and $H1000$) that describe return level curves (plots of extreme level versus the logarithm of the return period) that have too small a gradient (i.e. they are too 'flat', such as for Sitka, Aburatsu and Stockholm in Figure 1).

Figures 4 and 5 show comparisons between the two data sets using values from GESLA-2 and their nearest D-C locations. A maximum separation of 170 km between the centroid of a D-C segment and the tide gauge in GESLA-2 was allowed, which removed 26 of the 655 GESLA-2 records, and left 629

284 records. As mentioned above, the D-C segment centroids are mostly spaced apart by ~10 km. The
285 170 km separation cut was designed to exclude remote stations which are not represented in the D-
286 C data such as Antarctica and some remote islands.
287
288 Figure 4(a) shows a scatter plot of GESLA-2 vs. D-C scale parameters. Their differences have a
289 median of 0.024 m and a standard deviation of 0.071 m (Figure 4b). The distribution is best
290 described by the dashed line representing a least-squares fit through the origin, expressing D-C scale
291 parameters as 0.70 ± 0.02 times those from GESLA-2. This confirms our impressions from inspection
292 of Figures 3(a) and (b): most points do not lie on the diagonal, but the true scale parameters at these
293 locations, as provided by GESLA-2, are larger than the ones suggested by D-C. There is a very weak
294 correlation between the two sets (correlation coefficient = 0.196), corresponding to 4% of the
295 variance in D-C scale parameter values being explainable by the corresponding GESLA-2 values.
296
297 Figure 5(a) addresses the same topic, but in terms of the $H1$, $H10$, $H100$ and $H1000$ values at each
298 location instead of scale parameters. This figure allows us to make our second general point: that
299 the extreme levels ($H1$ to $H1000$), or the location parameters of the Gumbel distribution, in D-C
300 are too large when compared to GESLA-2. This bias could be explained by imprecise ocean tide
301 assumptions in D-C regarding the height of MHW above MSL, or, more likely, errors in the modelling
302 of the surge component of the extremes.
303
304 Figure 5(b) shows that in most cases the differences $H1000$ minus $H1$ in GESLA-2 are larger than in
305 D-C. This relates to our first general point: that the extreme level curves in D-C are too flat, as
306 previously demonstrated by the scale parameters in Figure 4(a).
307
308 Similar conclusions to those obtained from Figure 5 (a,b) can be drawn from complementary
309 cumulative distribution function (CCDF, also sometimes called the 'exceedance distribution') curves

of $H1$ etc. from the available sets of D-C and GESLA-2 information. Figure 5(c) shows the D-C CCDF curves for $H1$, $H10$, $H100$ and $H1000$ by lines in green, blue, red and black respectively. To their left, can be seen the set of four curves for GESLA-2, similarly coloured. For example, the black curve for D-C indicates that $H1000$ exceeds 4 m (above MSL) at approximately 20% of stations. On the other hand, the corresponding GESLA-2 black curve indicates that 20% of stations have values of $H1000$ exceeding only 3 m. Figure 5(c) can be inspected further to measure the spread of the $H1$-$H1000$ curves at their mid-points where the CCDF value is 0.5. The spread between the D-C distributions (green to black lines) at this mid-point is 0.59 m. This spread is more than 25% less than that in the GESLA-2 distributions (green to black lines) which is 0.80 m.

The same conclusions obtained from Figure 5(a-c) are found by requiring the GESLA-2 records to have at least 30 years of data rather than 20 years; in this case, 446 records are available, of which 435 remain after the 170 km separation requirement. The median difference between the two is 0.027 m, with a standard deviation of 0.069 m and a correlation coefficient of 0.284. At a CCDF value of 0.5, the spread of the D-C curves is 0.59 m, and that of the GESLA-2 curves is 0.86 m

It can be seen that Figure 5(c) allows us to make both of our general points, but in terms of the overall distribution of data rather than at individual locations: the D-C information contains sets of $H1$-$H1000$ values that on average are too large and with return level curves that are too 'flat' when compared to GESLA-2 observations.

4. Effects on Flood Impacts at Major Coastal Cities

As mentioned above, the point estimates of return water levels that we obtain from GESLA-2 cannot replace the D-C data in global impact models, such as DIVA, to explore the effects of the improved representation of extreme sea levels on exposure and risk estimates. However, we can use our

results and perform such analyses for a selection of large coastal cities using the model developed by Hallegatte et al. (2013; hereafter H13). In H13, present-day and future (under sea level rise and socio-economic scenarios) flood exposure and risk were assessed for the world's largest 136 port cities; extreme sea levels were taken from the D-C data set, as described above. Comparing the locations of these cities with those of the 655 tide gauges with more than 20 years of data in GESLA-2, we find that 59 (out of the 136) cities have a tide gauge within 200 km (Figure 6). Hence, for these 59 cities we can quantify the effects of the discrepancies between D-C and GESLA-2 on present-day and future exposure and risk estimates.

Figure 7 shows the relative differences (expressed in percentages) from using the D-C and GESLA-2 extreme sea levels in (i) present-day (here meaning the year 2005) exposure in terms of monetary assets to extreme sea levels with a return period of 100 years (Figure 7a), (ii) the present-day annual average losses (AAL) (Figure 7b), and (iii) the AAL in the year 2050 assuming 20 cm global sea level rise, 40 cm subsidence at cities that are subjected to subsidence, and socio-economic change (those are the same scenarios used in H13) (Figure 7c). For our sensitivity analysis we assume that no adaptation takes place until 2050. This is because defence standards in the H13 model are represented by return periods and hence the protection levels would change alongside our estimates of extreme sea levels. Most earlier analyses have made this assumption for consistency purposes. It is also worth noting that we focus on the relative comparison between results obtained with D-C and GESLA-2 data, rather than the absolute flood exposure and risk for individual cities.

In Figures 7(a) and 7(b) we can see that the average absolute differences for the present-day 100-year exposure and AAL are in the order of 20% and 30%, respectively. Using D-C data leads to an overestimation of both exposure and AAL at most cities, but coherent underestimation for cities in Europe, the only region where D-C extreme sea levels are generally too low. When we include sea level rise (Figure 7c) and assume no adaptation, the overestimation in AAL almost doubles to 57%

and occurs consistently in all regions. There are two notable exceptions in Australia (Brisbane and Sydney), where the scale parameters obtained from the D-C levels are larger than the ones from GESLA-2 (i.e. the Gumbel distributions from D-C have a steeper slope).

The above analysis shows us the overall effects of improving the representation of extreme sea level for the exposure and risk analysis. As outlined in the previous sections, there are different types of discrepancies between the D-C and GESLA-2 data, namely differences in the location parameters (leading to offsets in the return levels) and differences in the scale parameters (leading to different slopes of the distributions). In order to quantify the effects of each of these discrepancies, we modify the Gumbel distributions that we obtain from the GESLA-2 data. We start by removing the vertical offset, which means that at a particular site we move the GESLA-2 distribution upwards or downwards so that the 10-year return levels match the ones from the D-C data (we did the same for the 1-year events and the results were essentially the same). We then use the modified distributions and extreme sea level information to repeat the exposure and risk analysis (Figures 8a-c); this shows us the effect from having different slopes only. The differences in present-day 100-year exposure and AAL become much smaller (5% and 10% mean absolute differences) and now the D-C data leads generally to smaller values. This makes sense given that the modified distributions from GESLA-2 still have steeper slopes (at most sites) resulting in higher levels for long return periods (which are most important given that many cities have relatively high protection standards). Accordingly, there is still a significant overestimation of close to 50% when using D-C extremes and adding sea level rise; this is predominantly due to differences in the scale parameters (or distribution slopes).

Next, we go back to our original distributions obtained from the GESLA-2 data and this time we modify their slope to match the ones obtained from the D-C data. To achieve this, the distributions are rotated about the 1-year return period values. We then again repeat the exposure and risk analysis in order to quantify the effect from having only vertical offsets in the distributions (Figure

388 9a-c). For the present-day conditions the differences become much larger again (20% and 26% for
389 100-year exposure and AAL, respectively) and similar to those we found from the overall comparison
390 (Figure 7), but the mean absolute difference for AAL with sea level rise drops by almost half to 25%.
391
392 Based on these results we can make our third general point: that for present-day exposure and risk
393 assessments, discrepancies in the location parameters (or vertical offsets in the distributions) are
394 more important than discrepancies in the slopes, but when sea level rise is included discrepancies in
395 the scale parameters (or slopes of the distributions) clearly dominate in terms of distorting results
396 using the methods of H13, which are a standard approach for impact and risk models.
397
398 Despite the quantitative differences in 100-year exposure and AAL estimates, the absolute impacts
399 remain significant and the ranking of the cities that are most exposed and at risk from coastal
400 flooding changes little. Figure SM4 shows the ranking according to present-day AAL when using D-C
401 and GESLA-2 extremes. There is little change in the top 10 or top 20 of the 59 cities we were able to
402 analyse. Hence, the overall conclusions found here remain consistent with the insights presented in
403 H13.
404
405 5. Implications for Extreme Sea Level Frequencies with Sea Level Rise
406
407 Why do these differences between D-C and GESLA-2 matter? This can be answered by inspection of
408 Figure 10(a) which shows the increase in the frequency of extreme sea levels around the world if
409 MSL rises by 0.5 m, assuming that all other factors (tides, climatology of storm surges etc.) remain
410 the same in the future, and therefore that scale parameters remain the same. Such a rise in MSL
411 over the next 100 years is entirely plausible according to the IPCC AR5 (Church et al., 2013).
412

Figure 10(a) was made using D-C scale parameters derived using Equation 2. A Gumbel distribution will then imply an increase of $\exp\left(\frac{0.5}{\lambda}\right)$ in the frequency of a given level being exceeded for an 0.5 m MSL rise, with λ also in metres. It can be understood from this simple relationship why we chose to plot in Figure 3 the reciprocal of the scale parameter, as the quantity of most interest, rather than the scale parameter itself. In addition, it can be seen that, given a typical scale parameter of 0.1 m and an MSL rise of 0.5 m, then the increase in the frequency will be of the order of 150, and at locations where scale parameters are only a few centimetres (such as at some tropical islands or even at locations in the Mediterranean where the tidal range is small) almost any rise in MSL will lead to an extremely large increase in this frequency, and hence in the likelihood of flooding.

Figure 10(b) shows the corresponding distribution using the GESLA-2 information. This figure provides an update to Figure 13.25(a) in the IPCC AR5 and can be regarded as a set of 'true' values by means of which the worldwide distribution of Figure 10(a) can be validated. In fact, major differences can be seen between (a) and (b). The ratios of the increases in frequency from D-C compared to those using GESLA-2 information are shown in Figure 10(c), while their differences shown in Figure SM3 yield almost the same conclusion. Figures 10(c) and SM3 demonstrate in different ways that most coastlines would experience an increase in the likelihood of flooding (given an MSL rise of 0.5 m) that is much larger using D-C information than when using information from GESLA-2. This is also seen in the results from the city exposure and risk analysis for present-day and with future sea level rise.

6. Discussion and Conclusions

We have undertaken a validation of the extreme sea level information in the DINAS-COAST data set by means of comparison with information obtained from the tide gauge records in the GESLA-2 data set, and we have explored the implications for flood impact studies. Our three main points are:

(1) The extreme levels in D-C are systematically too 'flat' (i.e. they do not increase with return period as fast as the GESLA-2 observations).

(2) The extreme levels in D-C (i.e. the H values) are systematically larger than those in the GESLA-2 observations.

(3) Differences (or uncertainties) in location parameters are more important for present-day exposure and impact analysis, but differences in scale parameters dominate when future sea level rise is included.

Point 2 suggests that the D-C approach modelled either the extreme tide and/or storm surge components of extreme sea levels inadequately. One could definitely argue that using MHW will not represent the tidal extremes adequately. Mean high water springs (MHWS) would have been a better choice, and would have been as easily accessible a quantity to extract from tide tables as MHW. However, parameterising the tidal extremes by MHW or MHWS does not allow nodal and perigean tidal variations to be included in the extremes; this will be one reason why the D-C extreme levels are too flat.

However, using these arguments concerning inadequacies in the tidal extremes would also lead one to the conclusion that the extreme levels in D-C are too low on average, rather than too high, as the GESLA-2 data shows (i.e. Point 2). Consequently, we suspect that the main reason that the D-C H values are too high stems from the way that the storm surge contributions were computed.

461 The main consequence of having $H1$ to $H1000$ values that are too high (relative to MSL) is that the
462 present-day impact of flooding using a coastal database, in which heights are referred to a datum of
463 MSL, will be over-estimated; see our results from the city analysis. However, when coastal defences
464 and wider adaptation are considered, the situation is made more complex.
465
466 The main consequence of Point 1 is on studies of the change in likelihood of flooding when MSL
467 rises. Using the D-C data will overestimate the future growth in flood risk; for the cities we analysed
468 here there is an overestimation of more than 50%. Of course, this topic only considers one
469 component of impact and risk assessment (e.g. in our analysis we assume that no adaptation
470 occurs). Nevertheless, sea level extremes are an important component of such analyses.
471
472 Point 3 highlights that efforts should be undertaken to remove offsets and other biases from the
473 various representations of extreme sea level information such as in D-C (and for the newer ones
474 based on tide, surge and wave modelling mentioned below), in order to improve the quality of
475 present-day risk analyses; the new GESLA-2 data base can provide helpful insights on where such
476 biases exist and are most important. In particular, when the impacts of sea level rise are being
477 considered, it is important that the variability of extreme events is represented accurately in order
478 to obtain a realistic slope to the extreme value distribution (which, in our case, was a Gumbel but
479 which would be true for other parameterisations such as the GEV).
480
481 Overall, we have demonstrated that the improved data on sea level extremes from GESLA-2 clearly
482 point in the direction of obtaining lower estimates than those obtained in previous studies for the
483 exposure of people and assets to floods both today and in the future. An exploration of the H13
484 results suggests that, while their estimates of impacts will need to be reduced, the insights and
485 overall conclusions that emerge from that analysis are qualitatively robust. Of course, there is
486 continuing interest in obtaining firmer estimates of actual losses and adaptation costs. However, the

latter in particular are complex to calculate, which is why they have not been re-assessed in this paper.

Fortunately, improvements in large- to global-scale numerical modelling and related studies are allowing this to happen as illustrated by Muis et al. (2016), Vousdoukas et al. (2016) and other ongoing research. As these datasets on extremes become available, it is important that they be validated against a tide gauge data set such as GESLA-2, before being applied to new assessments that consider extreme sea levels with the other drivers of risk and exposure. In particular, it will be interesting to understand how an improved representation of extreme sea levels affects adaptation costs. As Wong et al. (2014) demonstrated, the costs of adaptation to sea level rise, particularly by developing countries, potentially represent enormous national investments: these assessments should be updated for the next IPCC assessment. Given the agreement at the Conference of Parties (COP)-21 in Paris in December 2015 to limit global warming to 2 degrees (and if possible to 1.5 degrees), a focus on hotspots for coastal impacts and adaptation needs, such as small islands and deltas would be especially important.

Acknowledgements

This work was undertaken when PLW was an Honorary Research Fellow at the National Oceanography Centre in Liverpool in receipt of an Emeritus Fellowship from the Leverhulme Trust. TW received funding from the European Union's Horizon 2020 research and innovation programme under the Marie Sklodowska-Curie grant agreement No 658025. RJN was supported by the European Commission's Seventh Framework Programme's collaborative project RISES-AM- (contract FP7-ENV-2013-two-stage-603396). Some of the figures in this paper were generated using the Generic Mapping Tools (Wessel and Smith, 1998).

513

514 References

515

516 Bosello, F., Nicholls, R.J., Richards, J., Roson, R., Tol, R.S.J., 2012. Economic impacts of climate
517 change in Europe: sea-level rise. Climatic Change 112, 63-81, doi:10.1007/s10584-011-0340-1.

518

519 Brown, S., Nicholls, R.J., Lowe, J.A., Hinkel, J., 2016. Spatial variations of sea-level rise and impacts:
520 An application of DIVA. Climatic Change 134, 403–416, doi:10.1007/s10584-013-0925-y.

521

522 Church, J.A., Clark, P.U. Cazenave, A., Gregory, J.M., Jevrejeva, S., Levermann, A., Merrifield, M.A.,
523 Milne, G.A., Nerem, R.S., Nunn, P.D., Payne, A.J., Pfeffer, W.T., Stammer, D., Unnikrishnan, A.S.,
524 2013. Sea Level Change. In: Stocker, T.F., D. Qin, G.-K. Plattner, M. Tignor, S.K. Allen, J. Boschung, A.
525 Nauels, Y. Xia, V. Bex and P.M. Midgley (eds.), Climate Change 2013: The Physical Science Basis.
526 Contribution of Working Group I to the Fifth Assessment Report of the Intergovernmental Panel on
527 Climate Change. Cambridge University Press, Cambridge, United Kingdom and New York, NY, USA.

528

529 Coles, S., 2001. An introduction to statistical modeling of extreme values. Springer, London. 208pp.

530

531 Diaz, D.B., 2016. Estimating global damages from sea level rise with the Coastal Impact and
532 Adaptation Model (CIAM). Climatic Change, 137-143, doi:10.1007/s10584-016-1675-4.

533

534 Hallegatte, S., Green, C., Nicholls, R.J., Corfee-Morlot, J., 2013. Future flood losses in major coastal
535 cities. Nature Climate Change 3, 802-806, doi:10.1038/NCLIMATE1979.

536

537 Hanson, S., Nicholls, R., Ranger, N., Hallegatte, S., Corfee-Morlot, J., Herweijer, C., Chateau, J., 2011.
538 A global ranking of port cities with high exposure to climate extremes. Climatic Change 104, 89-111,
539 doi:10.1007/s10584-010-9977-4.
540
541 Hinkel, J., Klein, R.J.T., 2009. Integrating knowledge to assess coastal vulnerability to sea-level rise:
542 The development of the DIVA tool. Global Environ. Chang. 19(3), 384–395,
543 doi:10.1016/j.gloenvcha.2009.03.002.
544
545 Hinkel, J., Nicholls, R.J., Vafeidis, A.T., Tol, R.S.J., Avagianou, T., 2010. Assessing risk of and
546 adaptation to sea-level rise in the European Union: an application of DIVA. Mitigation and
547 Adaptation Strategies for Global Change October 2010 15(7), 703–719, doi:10.1007/s11027-010-
548 9237-y.
549
550 Hinkel, J., Lincke, D., Vafeidis, A.T., Perrette, M., Nicholls, R.J., Tol, R.S.J., Marzeion, B., Fettweis, X.,
551 Ionescu, C., Levermann, A., 2014. Coastal flood damage and adaptation costs under 21st century
552 sea-level rise. P. Natl. Acad. Sci. 111, 3292-3297, doi:10.1073/pnas.1222469111.
553
554 Hoozemans, F.M.J., Marchand, M., Pennekamp, H.A., 1993. A global vulnerability analysis:
555 vulnerability assessment for population, coastal wetlands and rice production on a global scale. 2nd
556 Edition. Delft, The Netherlands: Delft Hydraulics.
557
558 Hunter, J., 2012. A simple technique for estimating an allowance for uncertain sea-level rise. Climatic
559 Change 113 239–252, doi:10.1007/s10584-011-0332-1.
560
561 Khouakhi, A., Villarini, G., 2016. Attribution of annual maximum sea levels to tropical cyclones at the
562 global scale. Int. J. Climatol. doi:10.1002/joc.4704.

563

564 Menéndez, M., Woodworth, P.L., 2010. Changes in extreme high water levels based on a quasi-
565 global tide-gauge dataset. J. Geophys. Res. 115, C10011, doi:10.1029/2009JC005997.

566

567 Merrifield, M.A., Genz, A.S., Kontoes, C.P., Marra, J.J., 2013. Annual maximum water levels from tide
568 gauges: Contributing factors and geographic patterns. J. Geophys. Res. Oceans 118, 2535-2546,
569 doi:10.1002/jgrc.20173.

570

571 McLeod, E., Hinkel, J., Vafeidis, A.T., Nicholls, R.J., Harvey, N., Salm, R., 2010. Sea-level rise
572 vulnerability in the countries of the Coral Triangle. Sustainability Science 5(2), 207-222,
573 doi:10.1007/s11625-010-0105-1.

574

575 Muis, S., Verlaan, M., Winsemius, H.C., Aerts, J.C.J.H., Ward, P.J., 2016. A global reanalysis of storm
576 surge and extreme sea levels. Nature Communications 7, 1-11, doi:10.1038/ncomms11969.

577

578 Nicholls, R.J., 2010. Impacts of and responses to sea-level rise. In Church, J. A., Woodworth, P. L.,
579 Aarup, T. and Wilson, W.S. (Eds.) Understanding sea-level rise and variability. Chichester, UK: Wiley-
580 Blackwell, pp. 17–51.

581

582 Nicholls R.J., Hoozemans, F.M.J., 2005. Global Vulnerability Analysis. In: M. Schwartz (ed.)
583 Encyclopaedia of Coastal Science, Kluwer Academic Publishers, Dordrecht, Netherlands, pp. 486-491.
584 link.springer.com/referencework/10.1007%2F1-4020-3880-1.

585

586 Nicholls, R.J., Marinova, N., Lowe, J.A., Brown, S., Vellinga, P., de Gusmo, D., Hinkel, J., Tol, R.S.J.,
587 2011. Sea-level rise and its possible impacts given a 'beyond 4C world' in the twenty-first century.
588 Philos. T. Roy. Soc. A 369, 161-181, doi:10.1098/rsta.2010.0291.

589

590 Pardaens, A.K., Lowe, J.A., Brown, S., Nicholls, R.J., de Gusmo, D., 2011. Sea-level rise and impacts
591 projections under a future scenario with large greenhouse gas emission reductions. Geophys. Res.
592 Lett. 38, L12604, doi:10.1029/2011GL047678.

593

594 Pugh, D., Woodworth, P., 2014. Sea-level science: Understanding tides, surges, tsunamis and mean
595 sea-level changes. Cambridge: Cambridge University Press. ISBN 978-1-107-02819-7. 395pp.

596

597 R Development Core Team, 2011. R: a language and environment for statistical computing. R
598 Foundation for Statistical Computing, Vienna, Austria. http://www.R-project.org, ISBN 3-900051-07-
599 0.

600

601 Vafeidis, A.T., Nicholls, R.J., McFadden, L., Tol, R.S.J., Hinkel, J., Spencer, T., Grashoff, P.S., Boot, G.,
602 Klein, R.J.T., 2008. A new global coastal database for impact and vulnerability analysis to sea-level
603 rise. J. Coastal Res. 24(4), 917–924, doi: 10.2112/06-0725.1.

604

605 van den Brink, H.W, Können, G.P, 2011. Estimating 10000-year return values from short time series.
606 Int. J. Climatol. 31(1), 115–126, doi:10.1002/joc.2047.

607

608 von Storch, H., Woth, K., 2008. Storm surges: perspectives and options. Sustainability Science 3, 33–
609 43, doi:10.1007/s11625-008-0044-2.

610

611 Vousdoukas, M. I., Voukouvalas, E., Mentaschi, L., Dottori, F., Giardino, A., Bouziotas, D., Bianchi, A.,
612 Salamon, P., Feyen, L., 2016. Developments in large-scale coastal flood hazard mapping. Nat.
613 Hazards Earth Syst. Sci. 16, 1841-1853, doi:10.5194/nhess-16-1841-2016.

614

615 Wessel, P., Smith, W.H.F., 1998. New, improved version of Generic Mapping Tools released. EOS,
616 Trans. AGU 79, 579.
617
618 Wolff, C., Vafeidis, A.T., Lincke, D., Marasmi, C., Hinkel, J., 2016. Effects of scale and input data on
619 assessing the future impacts of coastal flooding: an application of DIVA for the Emilia-Romagna
620 coast. Front. Mar. Sci. 3, 41, doi: 10.3389/fmars.2016.00041.
621
622 Wong, P.P., Losada, I.J., Gattuso, J.-P., Hinkel, J., Khattabi, A., McInnes, K.L., Saito, Y., Sallenger, A.,
623 2014. Coastal systems and low-lying areas. In: Field, C.B., V.R. Barros, D.J. Dokken, K.J. Mach, M.D.
624 Mastrandrea, T.E. Bilir, M. Chatterjee, K.L. Ebi, Y.O. Estrada, R.C. Genova, B. Girma, E.S. Kissel, A.N.
625 Levy, S. MacCracken, P.R. Mastrandrea, and L.L.White (eds.), Climate Change 2014: Impacts,
626 Adaptation, and Vulnerability. Part A: Global and Sectoral Aspects. Contribution of Working Group II
627 to the Fifth Assessment Report of the Intergovernmental Panel on Climate Change. Cambridge
628 University Press, Cambridge, United Kingdom and New York, NY, USA, pp. 361-409.
629
630 Woodworth, P.L., Hunter, J.R., Marcos, M., Caldwell, P., Menéndez, M., Haigh, I., 2017. Towards a
631 global higher-frequency sea level data set. Geoscience Data Journal, (in press), doi:10.1002/gdj3.42.
632

633

634 Figure Captions

635

636 1. Annual maximum sea levels (above MSL) plotted versus return period observed at stations in
637 quite different locations: Sitka, Alaska, United States; Aburatsu, Japan; Charleston, South Carolina,
638 United States; Stockholm, Sweden; Isla Fiscal, Rio de Janeiro, Brazil; Fremantle, Australia. The dashed
639 lines give 95% confidence intervals for the linear Gumbel fits. The black squares are the $H1$, $H10$ and
640 $H100$ values (above MSL) for this location in the D-C data set.

641

642 2. Number of annual maximum sea levels used in the final Gumbel fits in method 1. Only records
643 with more than 20 annual maxima are shown and are used in the subsequent analysis.

644

645 3. Reciprocal (m^{-1}) of the Gumbel scale parameter (a) at each point on the world coastline in the D-C
646 data set using $H1$ and $H100$ to compute the scale parameters, and (b) for records in GESLA-2 with
647 at least 20 years of data.

648

649 4. (a) Scale parameters in D-C and GESLA-2 at the tide gauge locations in the GESLA-2 set. The solid
650 line indicates the (1:1) diagonal while the dashed line shows a least-squares linear relationship
651 passing through the origin. (b) The difference between GESLA-2 and D-C scale parameters.

652

653 5. (a) Extreme levels (above MSL) for 1, 10, 100 and 1000 year return periods (green, blue, red and
654 black respectively) in D-C and GESLA-2; (b) Differences between $H1000$ and $H1$ in D-C and GESLA-
655 2; (c) Complementary cumulative distribution function (CCDF) curves of the 1, 10, 100 and 1000 year
656 return period extreme levels (green, blue, red and black respectively) in D-C and GESLA-2 at the tide
657 gauge locations in the GESLA-2 set. For each return period (or colour) there are 2 curves, with that
658 for D-C being to the right (higher return level for given CCDF value) of that for GESLA-2.

6. Data availability (the colourbar indicating the number of annual maxima) at sites where tide gauges are located close (see size of circles) to cities analysed by Hallegate et al. (2013); black dots denote cities where no tide gauges are close by or do not provide sufficient data (see text).

7. Relative differences in (a) exposure of monetary assets to a 100-year extreme sea level event, (b) annual average losses under 2005 conditions, and (c) annual average losses for 2050 with sea level rise and no adaptation when using GESLA-2 and D-C extreme estimates; blue indicates that results based on D-C are too small, red means they are too high. Relative differences are expressed as (Value using D-C minus Value using GESLA)/Value using D-C.

8. Same as Figure 7, but the GESLA-2 offsets for 10-year return levels were removed to match the D-C results.

9. Same as Figure 7, but the slopes in the GESLA-2 return level estimates were adjusted to match the D-C results.

10. Increases in the frequency of extreme sea levels if mean sea level rises by 0.5 m using (a) D-C and (b) GESLA-2 information. The colour scales saturate at 1000 for consistency with Figure 13.25(a) of Church et al. (2013). (c) Ratio of the increases in frequency for D-C and those for GESLA-2, under 0.5 m of mean sea level rise.

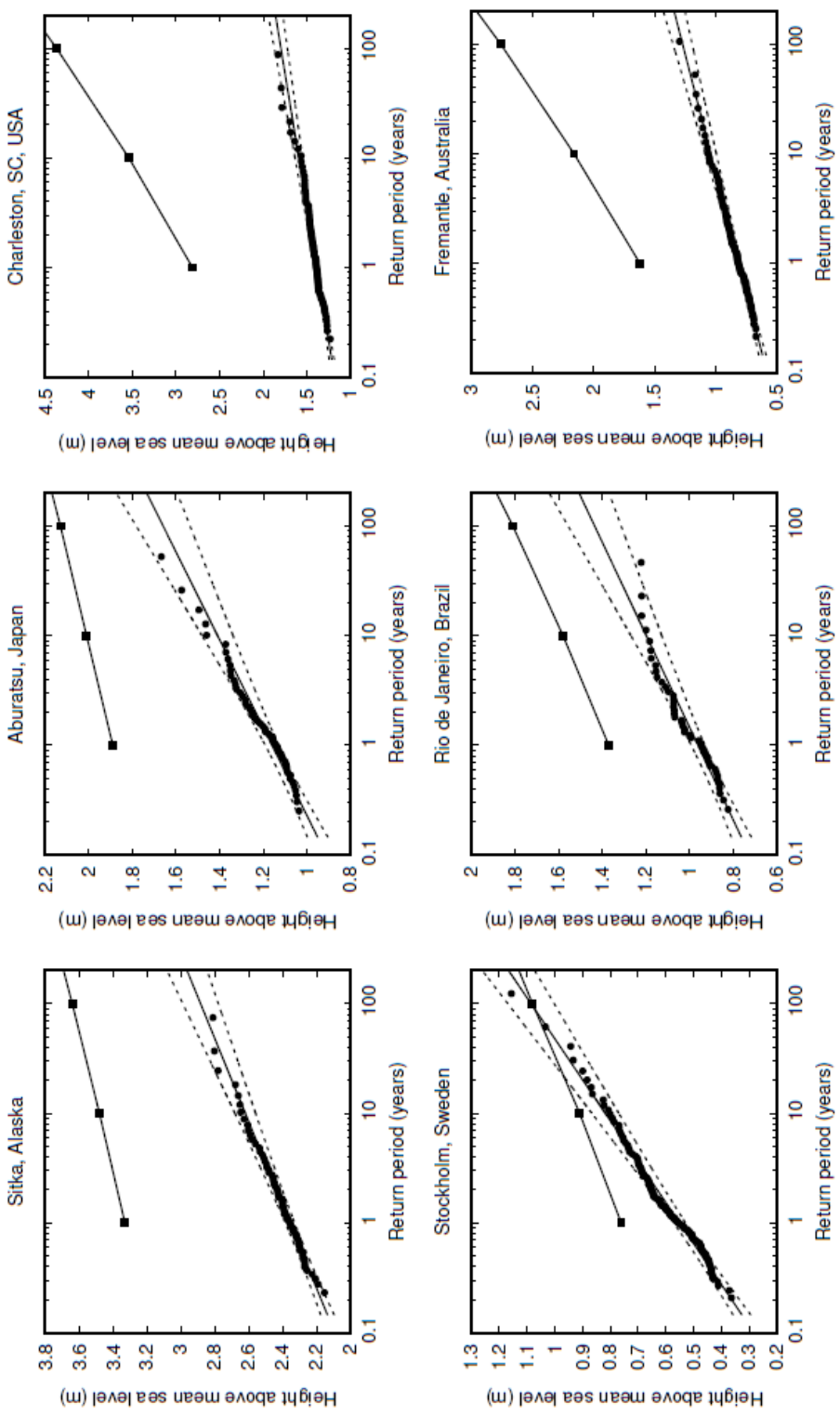
Charleston, SC, USA
Fremantle, Australia
Aburatsu, Japan
Rio de Janeiro, Brazil
Sitka, Alaska
Stockholm, Sweden
Height above mean sea level (m)
Return period (years)

Figure 1

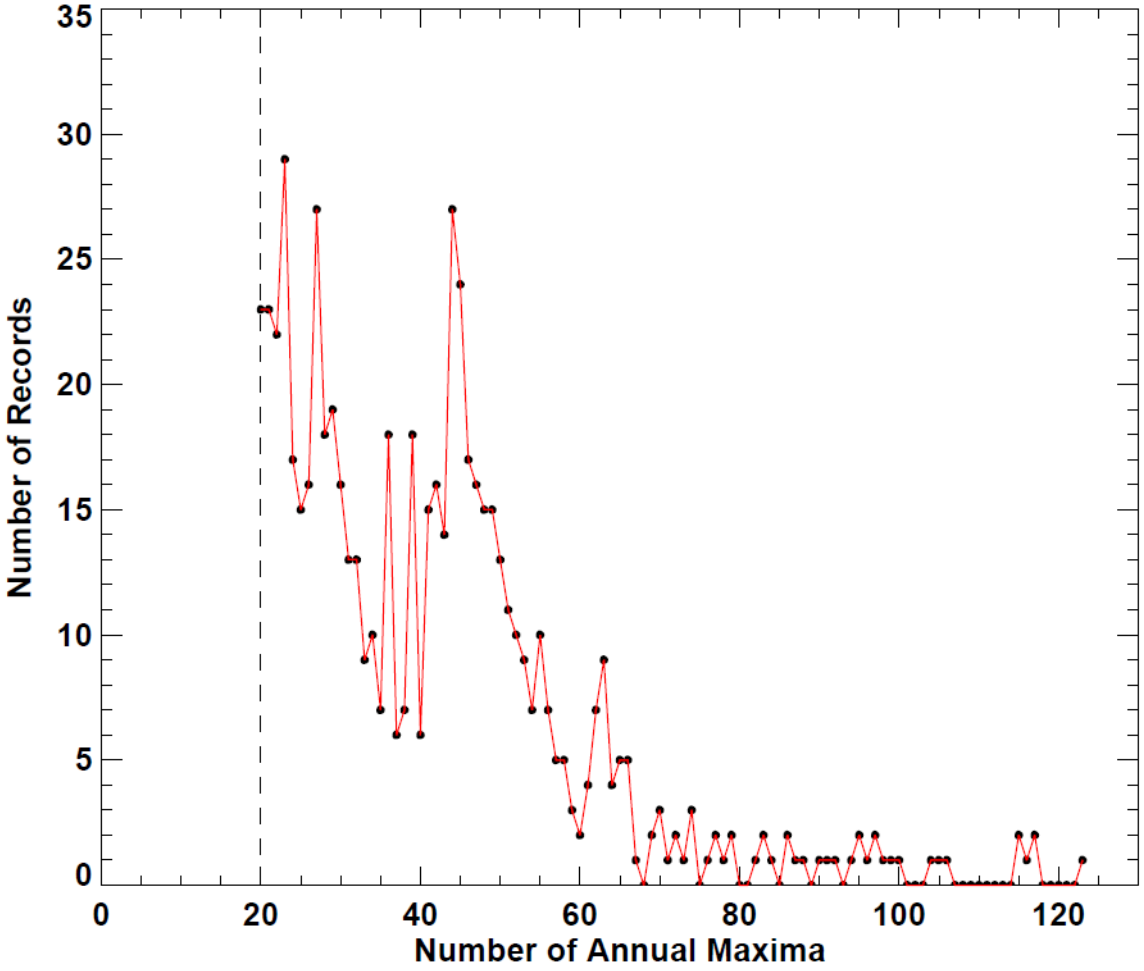
Number of Records
Number of Annual Maxima
0
5
10
15
20
25
30
35
0
20
40
60
80
100
120

Figure 2

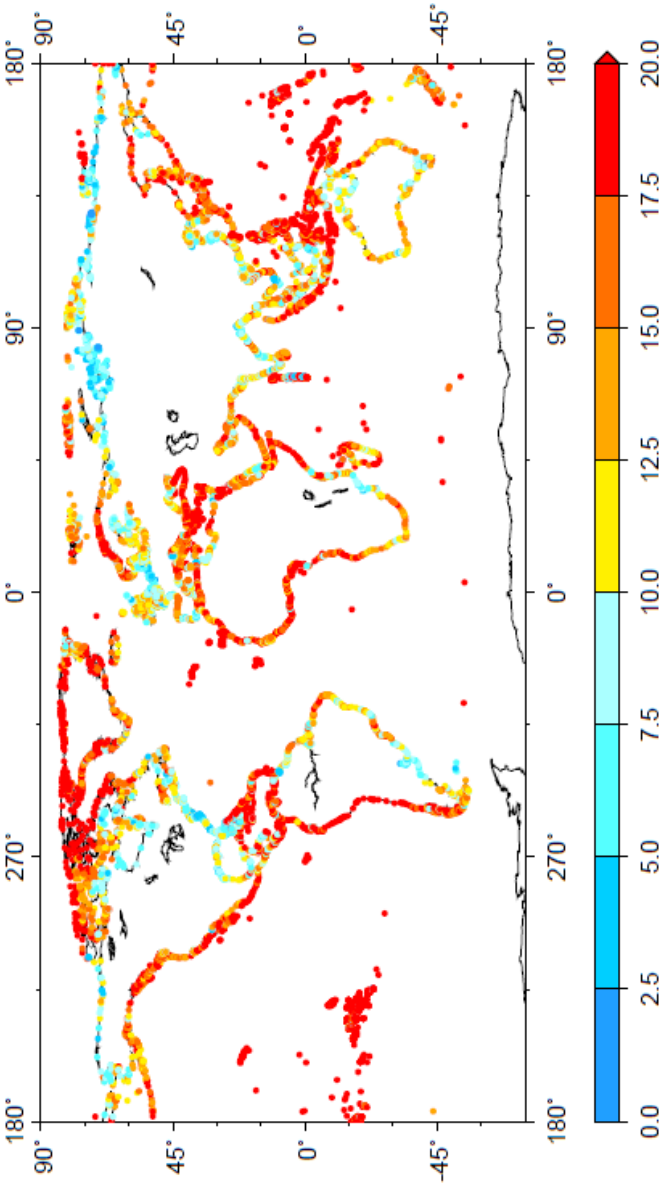

688 Fig.3a
689

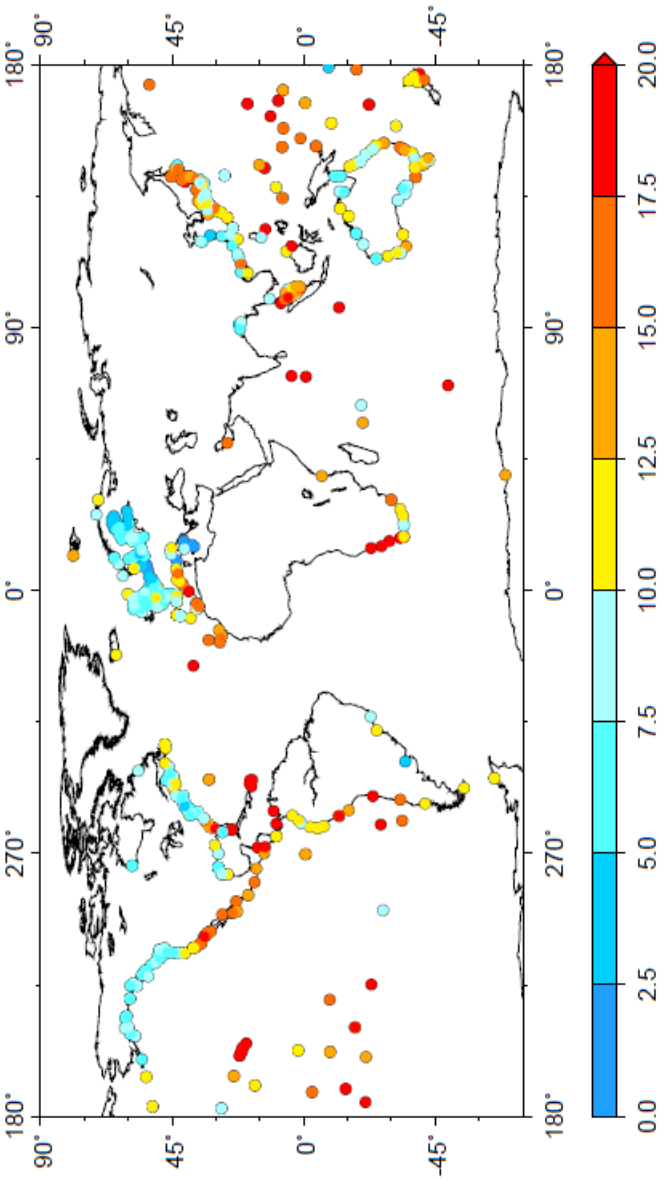

690 Fig.3b

691

692

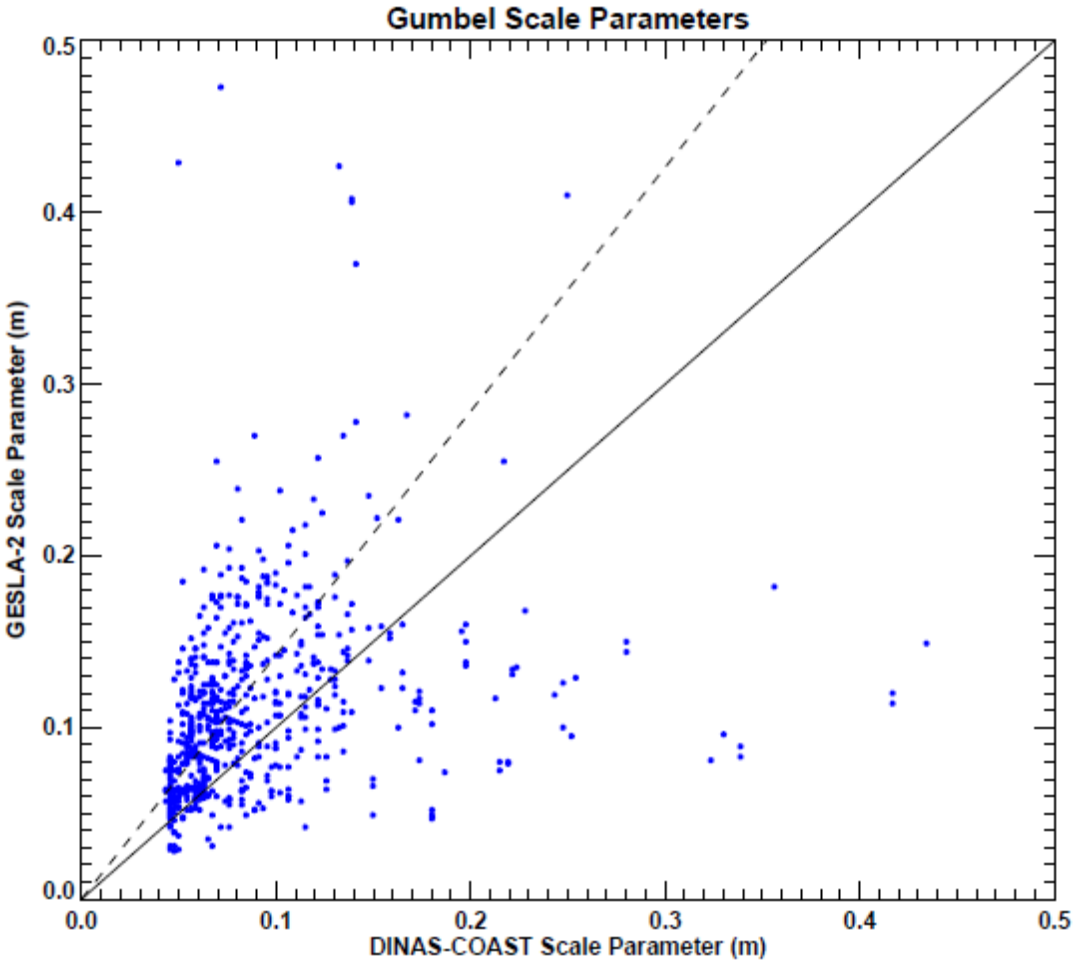

693
694
695 Figure 4a
696

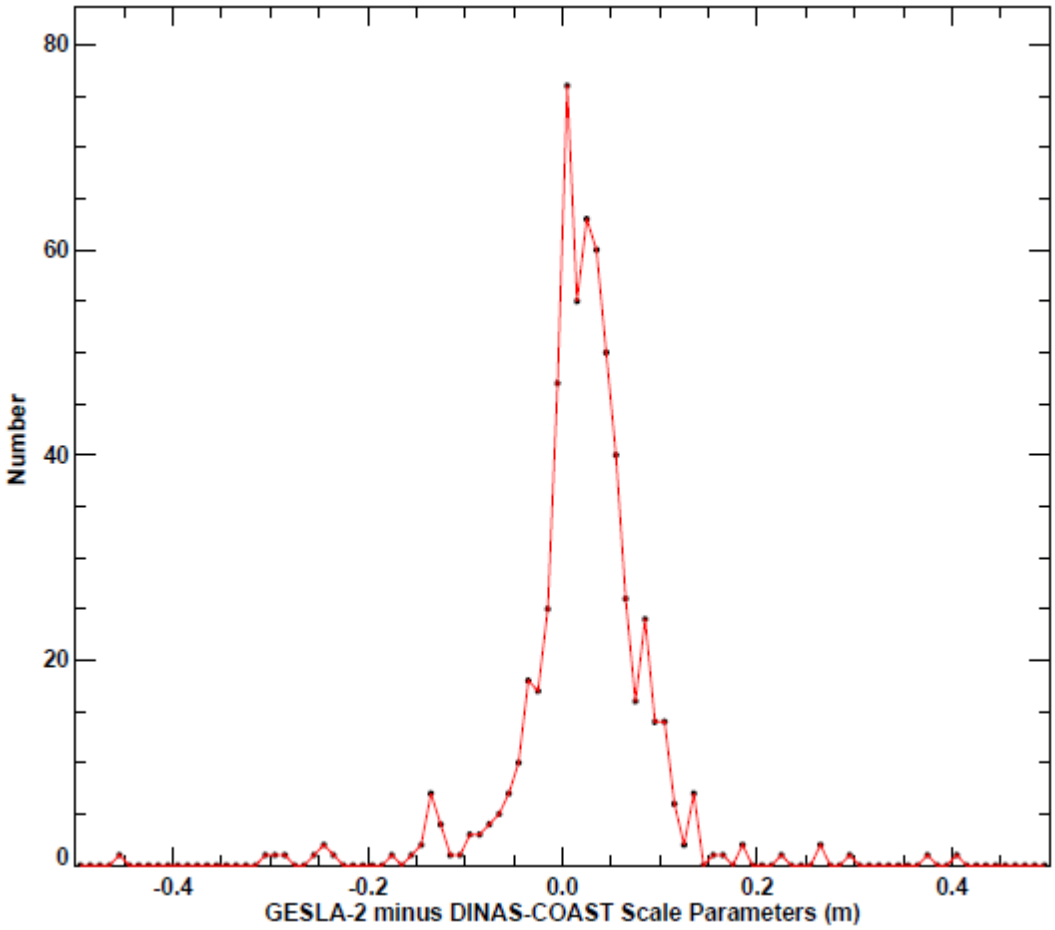
80
60
40
20
0
Number
-0.4
-0.2
0.0
0.2
0.4
GESLA-2 minus DINAS-COAST Scale Parameters (m)

Figure 4b

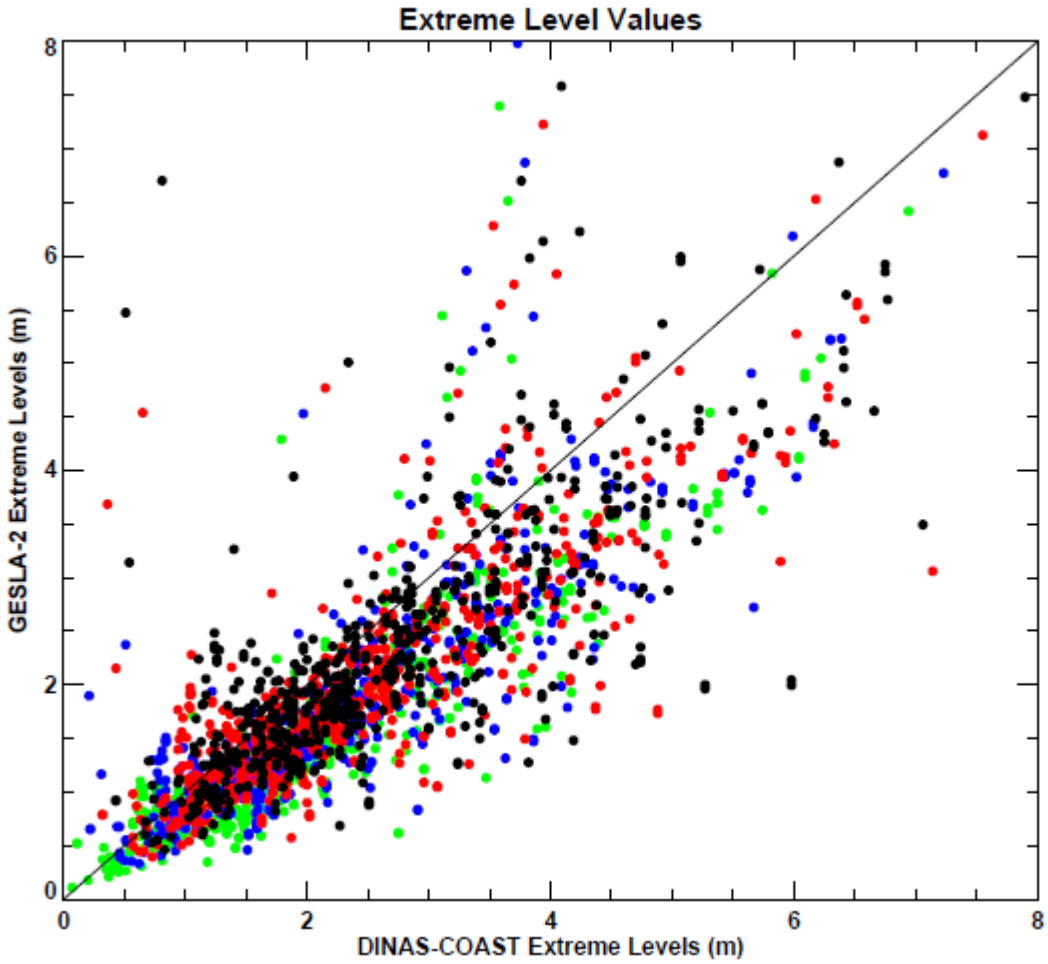

701
702 Figure 5(a)
703

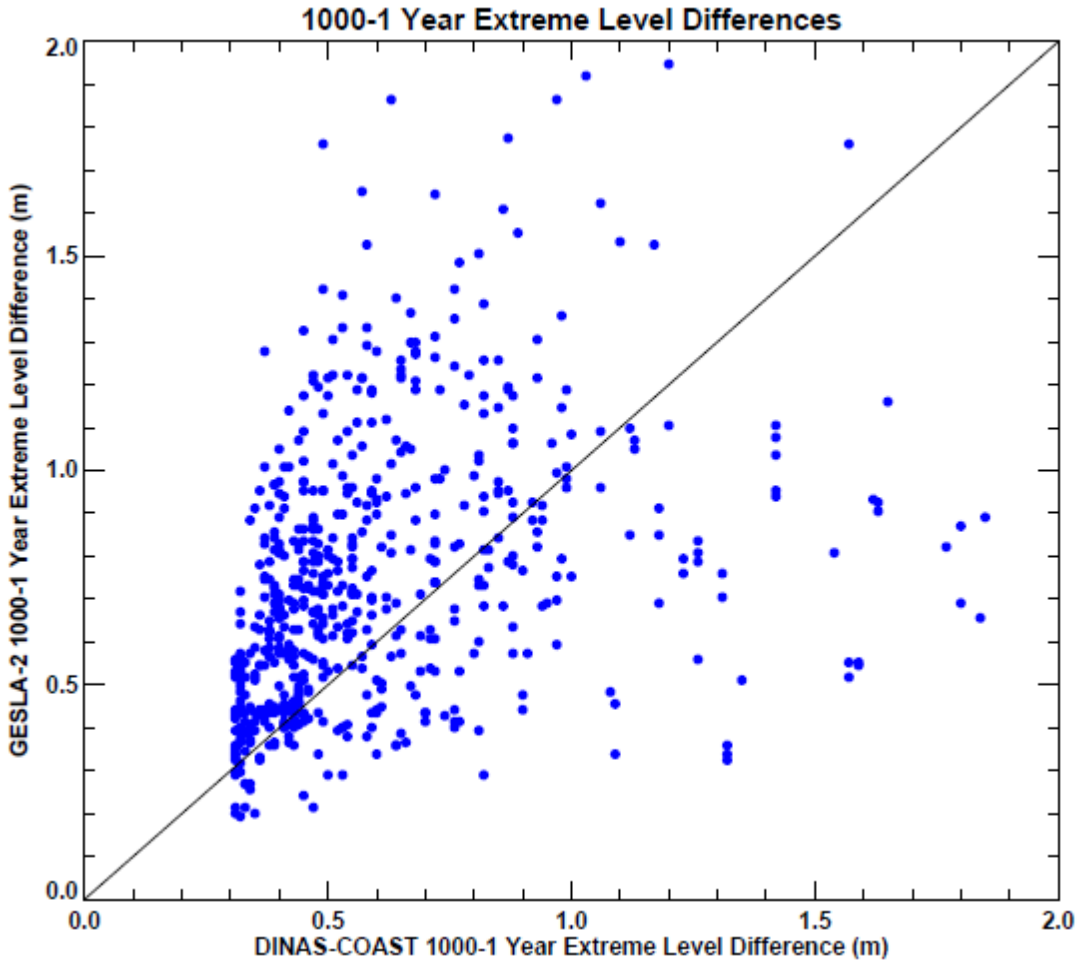
1000-1 Year Extreme Level Differences
GESLA-2 1000-1 Year Extreme Level Difference (m)
DINAS-COAST 1000-1 Year Extreme Level Difference (m)
0.0
0.5
1.0
1.5
2.0

Figure 5(b)

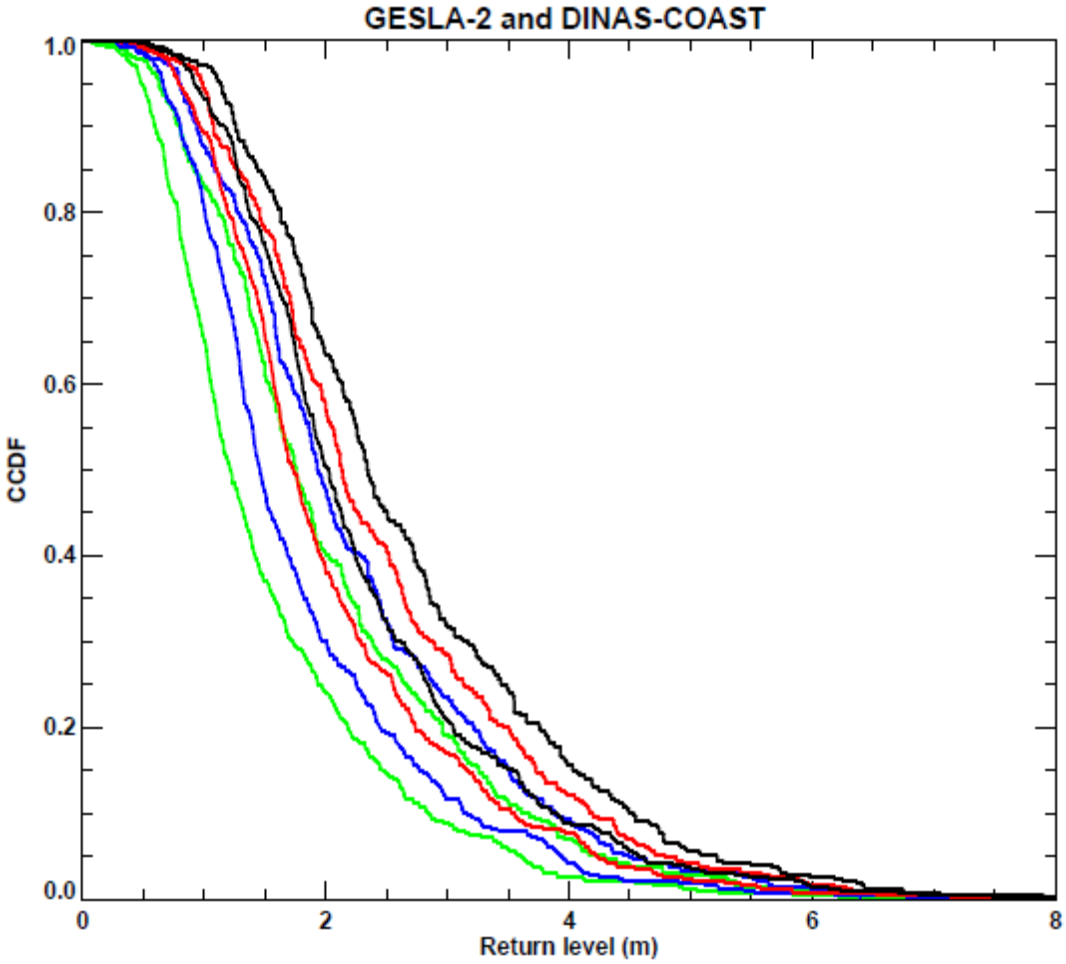

708
709
710 Figure 5(c)
711

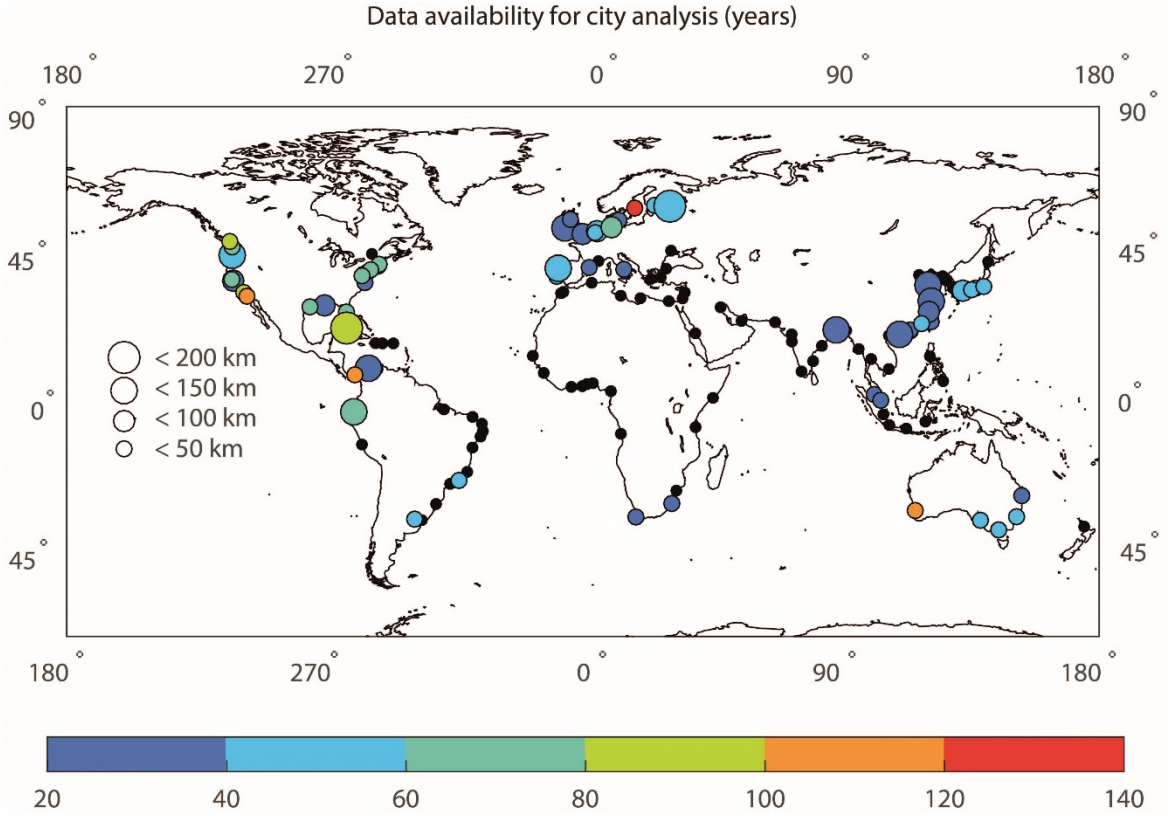

712

713 Figure 6

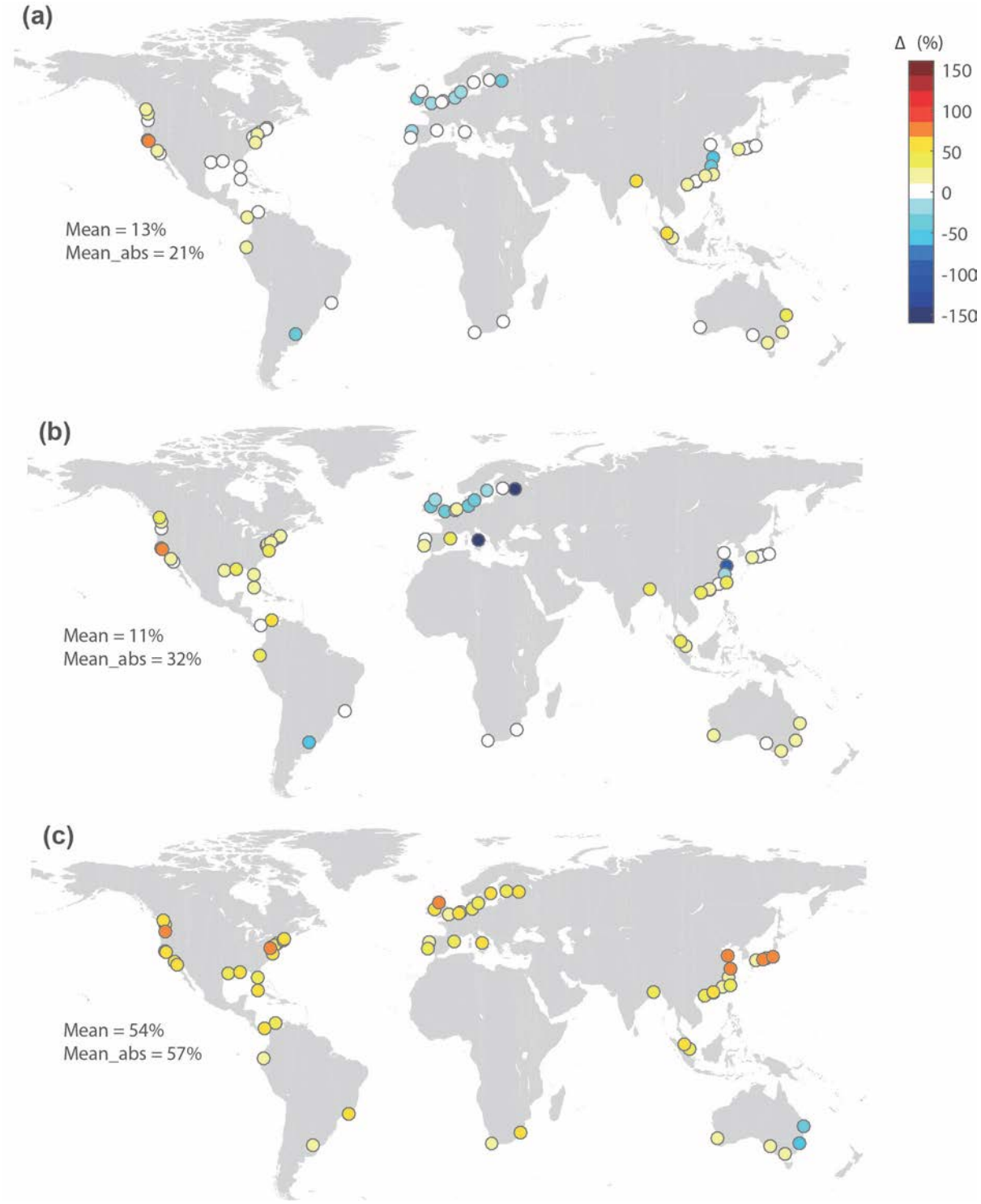

714

715 Figure 7

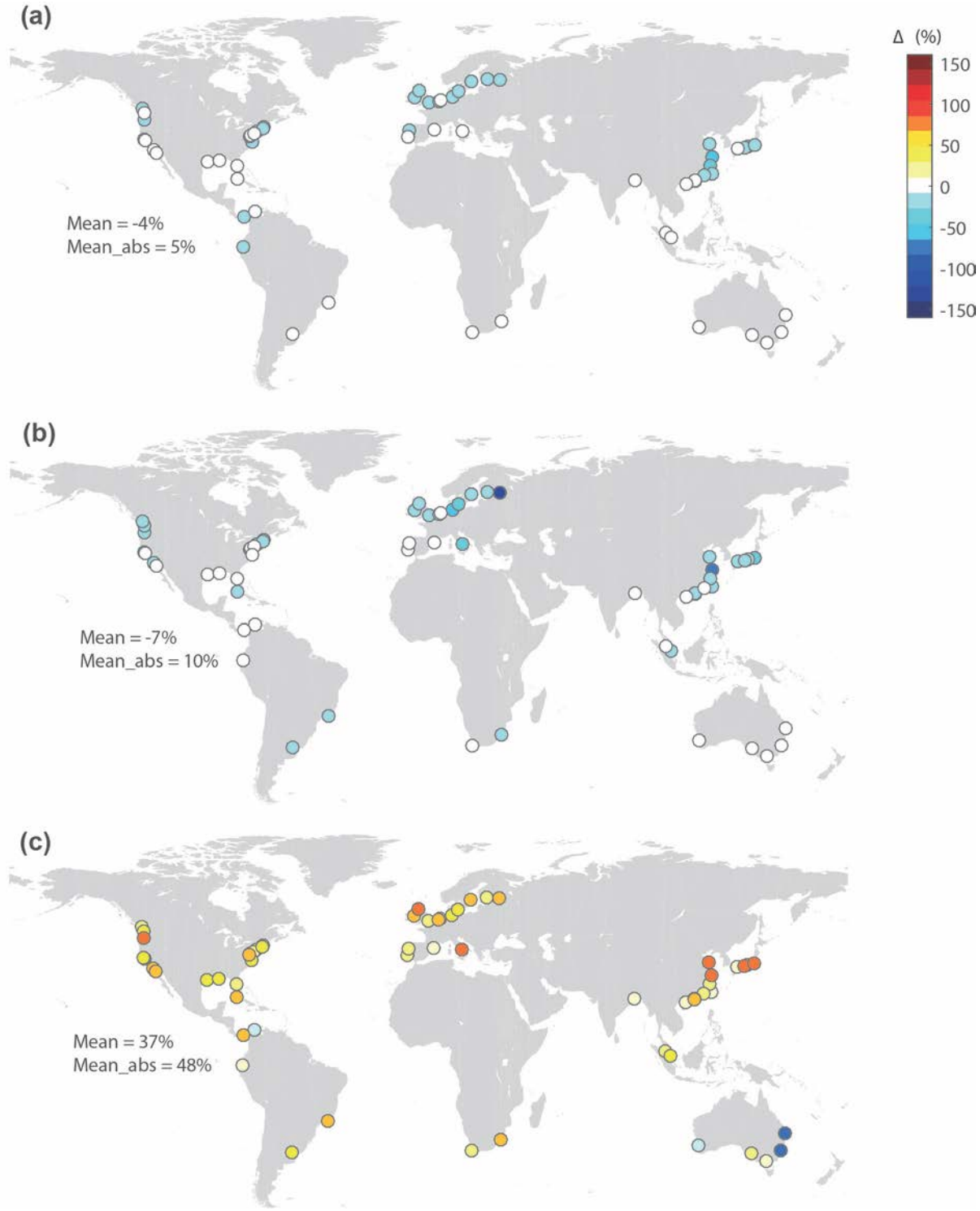

716

717 Figure 8

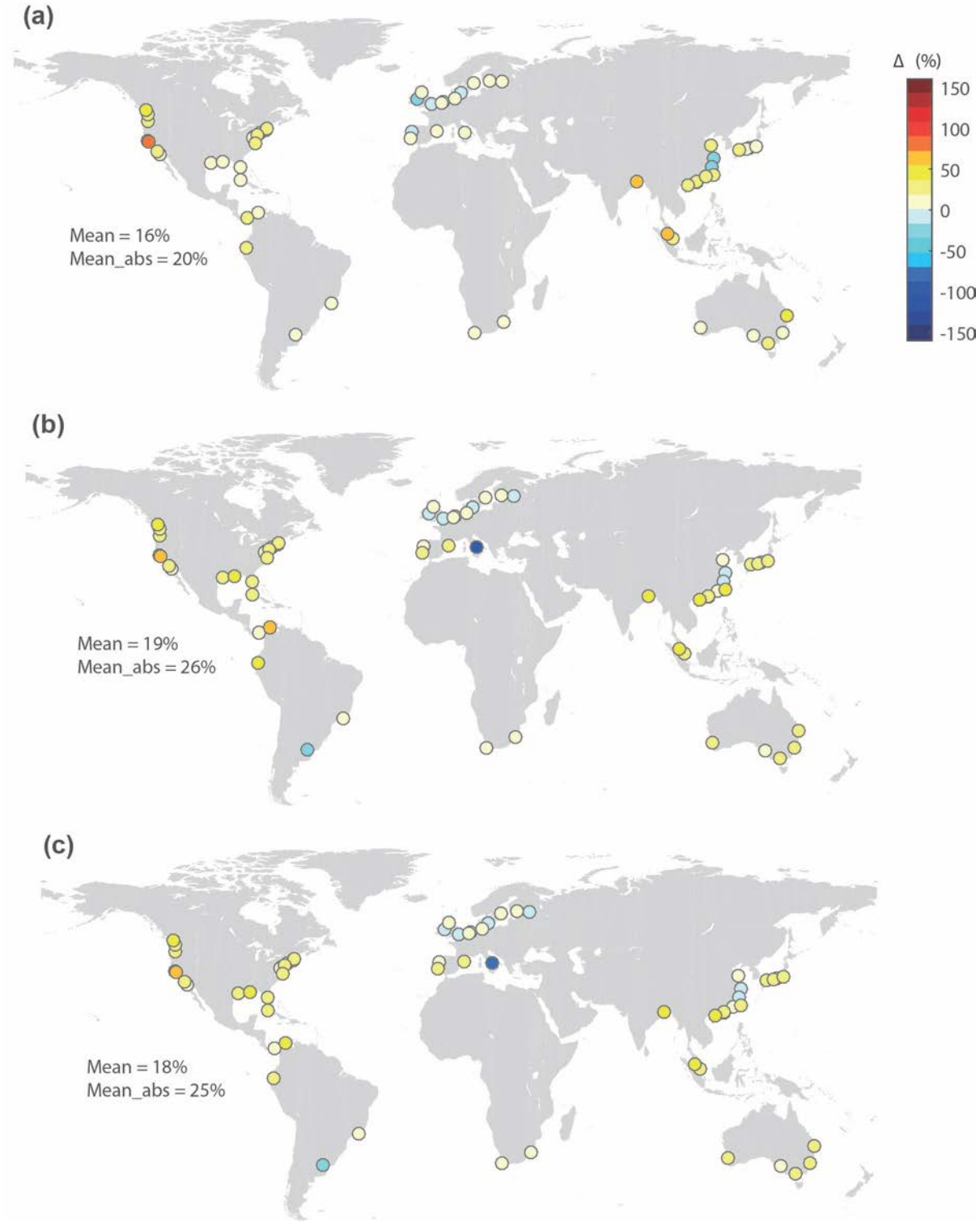

718

719 Figure 9

720

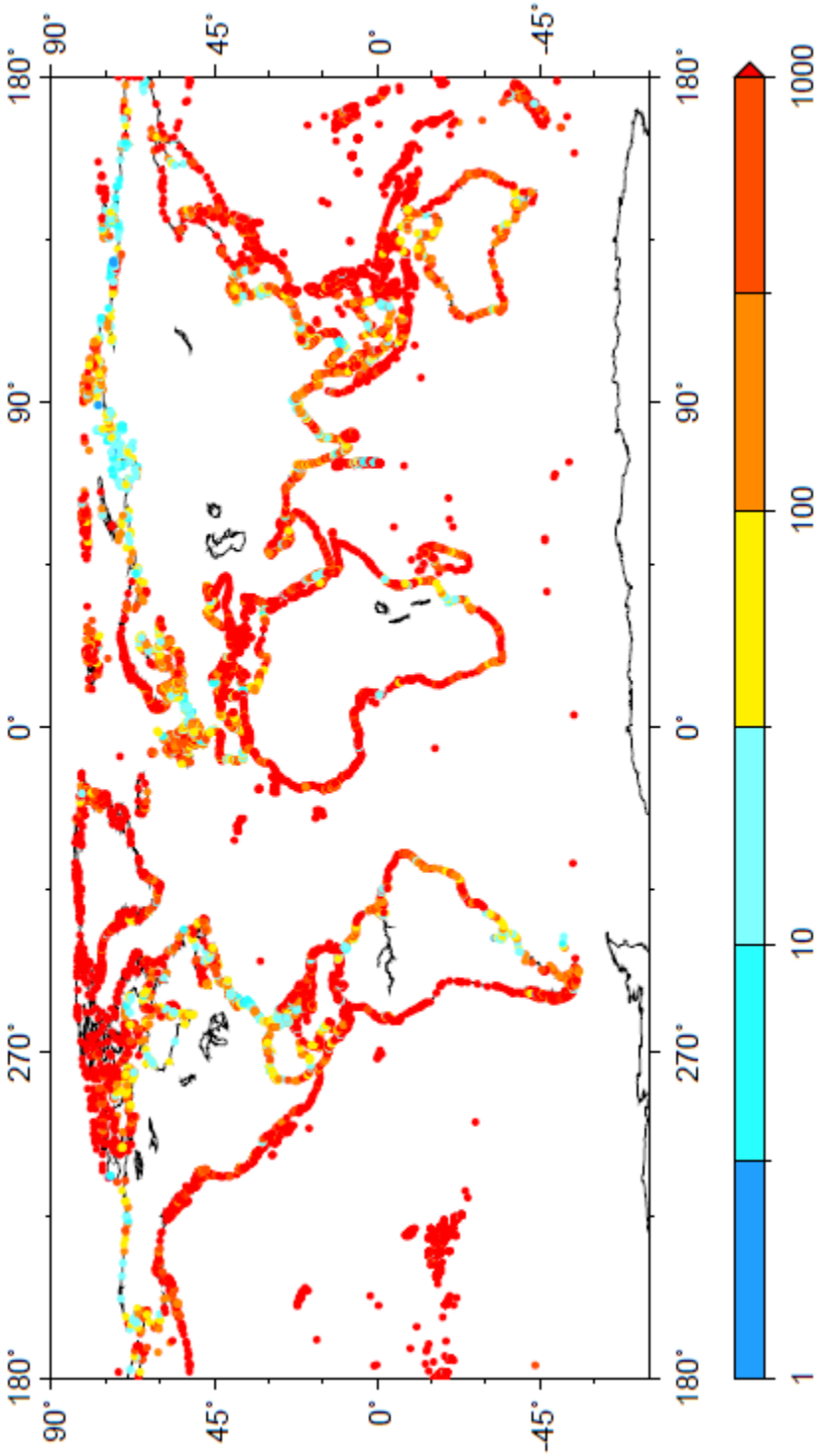

721 Fig.10a
722

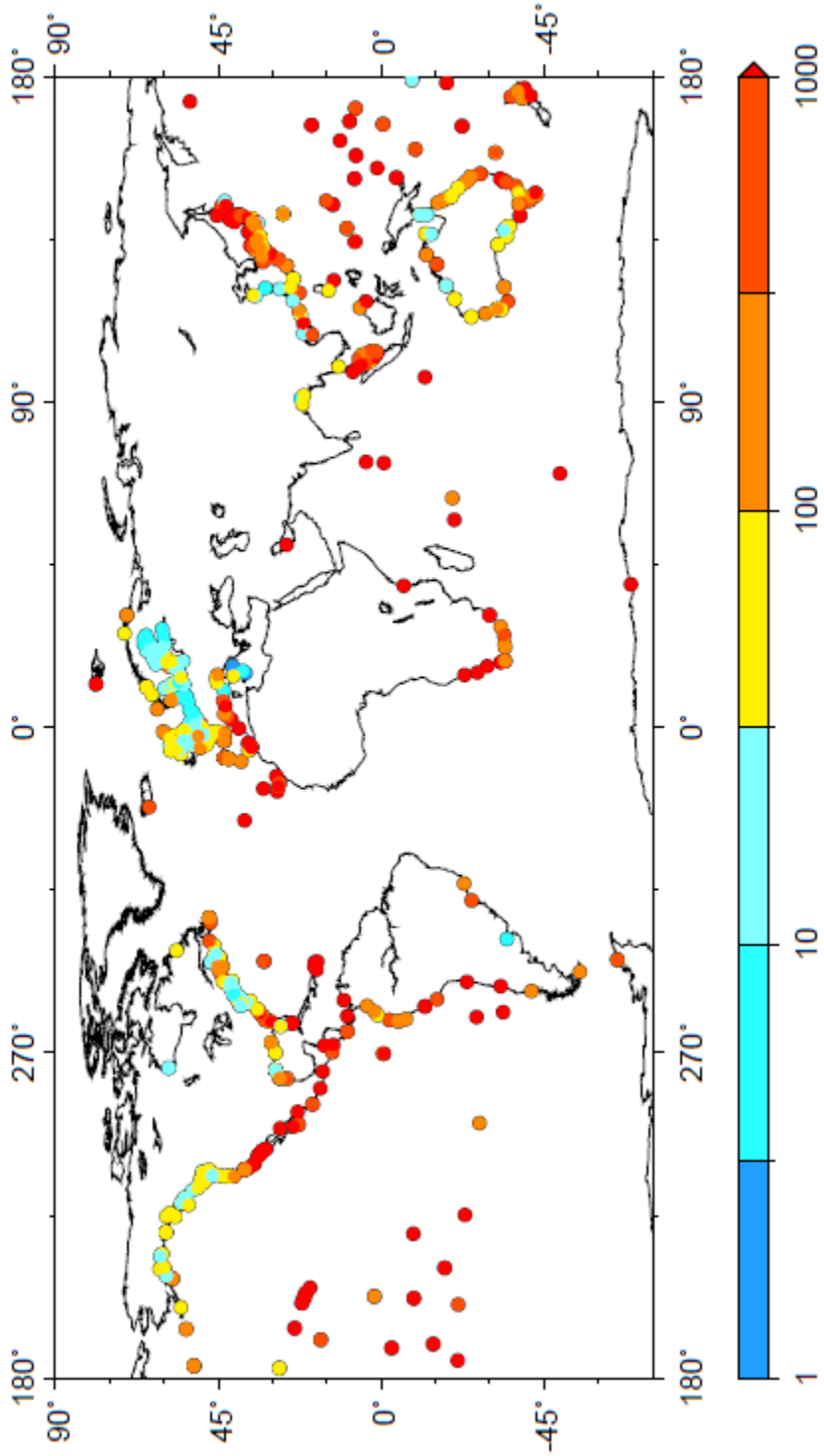

723
724 Fig.10b

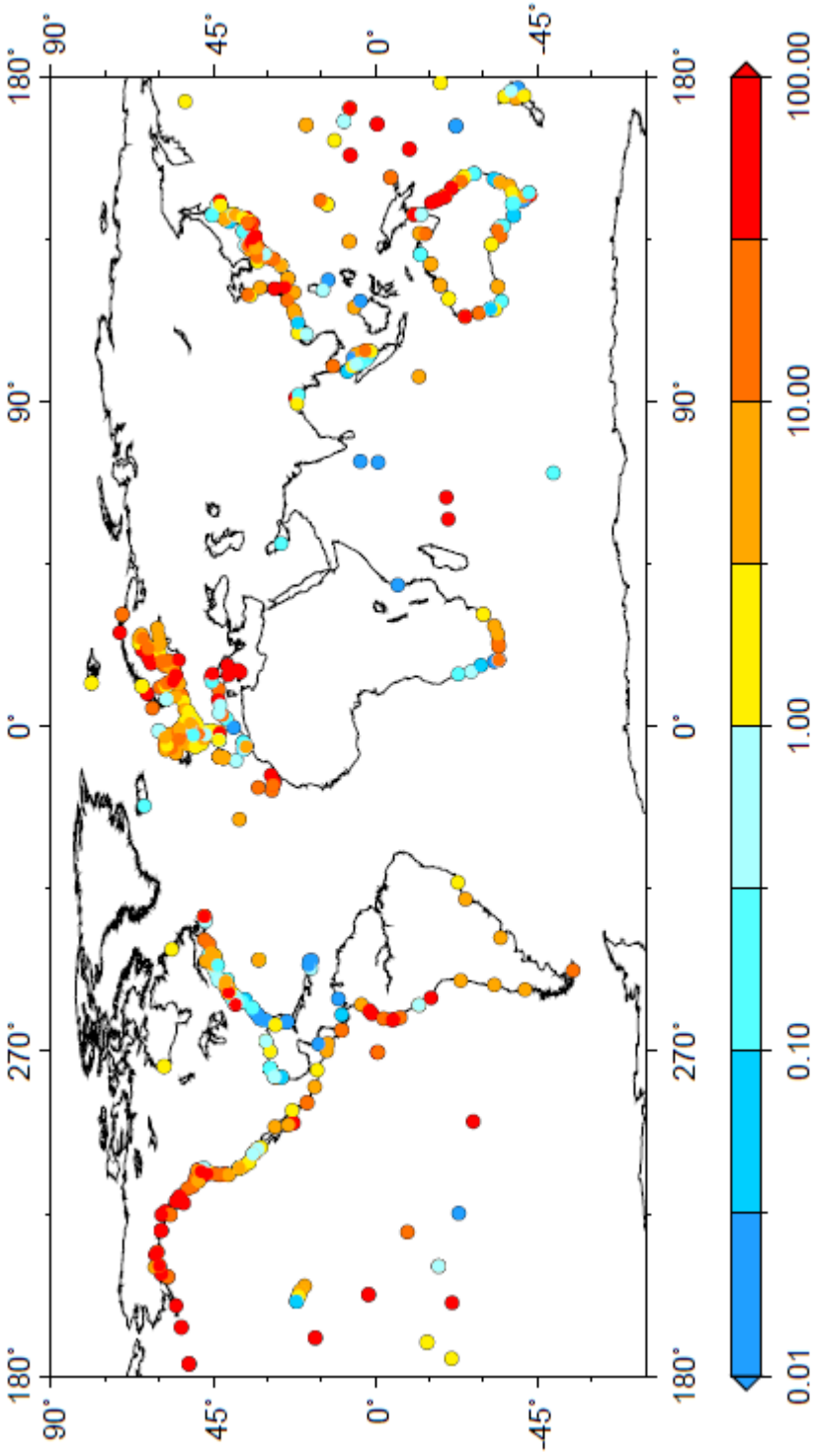
180°
90°
45°
0°
-45°
180°
90°
0°
270°
180°
90°
45°
0°
-45°
180°
90°
0°
270°
180°
100.00
10.00
1.00
0.10
0.01

Fig 10c